Fan et al. Phytopathology Research (2019) 1:11
https://doi.org/10.1186/s42483-019-0019-5

Phytopathology Research

RESEARCH Open Access

A core effector UV_1261 promotes *Ustilaginoidea virens* infection via spatiotemporally suppressing plant defense

Jing Fan[1†], Ning Du[1†], Liang Li[1†], Guo-Bang Li[1], Yu-Qiu Wang[1,5], Yu-Feng Zhou[3], Xiao-Hong Hu[1], Jie Liu[1], Ji-Qun Zhao[1], Yan Li[1], Fu Huang[3,4] and Wen-Ming Wang[1,2*]

Abstract

False smut is a destructive grain disease of rice worldwide, characterized by false smut balls formed in rice flowers. Here we identified a small secreted protein UV_1261 contributing to virulence of *Ustilaginoidea virens*, the causal agent of this disease. The sequence of *UV_1261* was highly conserved among isolates of *U. virens* and absent in other fungi. *UV_1261* encodes a protein targeted to plant chloroplasts. Its expression exhibited a bimodal pattern during pathogenesis. Ectopic expression of *UV_1261* in *Nicotiana benthamiana* and Arabidopsis led to suppression of flg22-induced ROS burst, callose deposition, and expression of defense-related genes, as well as enhanced susceptibility to powdery mildew in Arabidopsis. Down-regulation of *UV_1261* via exogenous siRNA treatment resulted in reduced number of false smut balls. Consistently, stably knocking-down *UV_1261* caused less number of false smut balls associated with higher expression of defense-related genes in rice flower. Taken together, our data demonstrate that UV_1261 is a core effector of *U. virens* essential for virulence and suppressing defense in rice flower, and thus may serve as a potential molecular target for controlling rice false smut disease.

Keywords: Defense, Effector, Pathogenicity, Rice false smut, siRNA, *Ustilaginoidea virens*

Background

Flower is a nutrient-rich sink organ, attracting habitation of a large number of microorganisms. Flower-infecting fungi have caused diseases in many economically important crops. For example, *Claviceps purpurea* causes ergot disease in rye and *Gibberella zeae* causes Fusarium head blight in wheat (Ngugi and Scherm 2006). In recent years, rice false smut (RFS) disease, caused by the flower-infecting pathogen *Ustilaginoidea virens*, has emerged as a serious grain disease worldwide (Fan et al. 2016). Occurrence of RFS disease not only leads to yield loss, but also contaminates grains and straws with mycotoxins that are poisonous to both human and animals (Koiso et al. 1994; Nakamura et al. 1994). However, our understanding on the pathogenesis of this disease is very limited.

In recent years, several groups independently reported the infection process of *U. virens* in rice flower and a few genes have been identified to be involved in the process (Ashizawa et al. 2012; Tang et al. 2013; Hu et al. 2014; Fan et al. 2015; Song et al. 2016). Generally, the infection process can be divided into two stages. In stage I, conidia of *U. virens* germinate on the surface of rice spikelet, and generate hyphae or mycelia that grow epiphytically (Ashizawa et al. 2012; Fan et al. 2012). In stage II, mycelia extend into the inner space of spikelet via the gap between the lemma and the palea (Ashizawa et al. 2012), firstly attack stamen filament (Tang et al. 2013), then infect lodicule, stigma and style (Song et al. 2016; Yong et al. 2016), and ultimately embrace all the floral organs to form a ball-shape colony called false smut ball (Tang et al. 2013; Fan et al. 2015). Stage I lasts for 3–5 days, while stage II 7–10 days (Tang et al. 2013; Fan et al. 2015). In addition, a few genes have been found to be associated with infection of *U. virens*

* Correspondence: j316wenmingwang@sicau.edu.cn
Jing Fan, Ning Du and Liang Li contributed equally to the work.
[1]Rice Research Institute, Sichuan Agricultural University, 211 Huimin Road, Wenjiang District, Chengdu 611130, China
[2]Collaborative Innovation Center for Hybrid Rice in Yangtze River Basin, Sichuan Agricultural University, 211 Huimin Road, Wenjiang District, Chengdu 611130, China
Full list of author information is available at the end of the article

in rice. For example, *UvPRO1* encodes a C6 transcription factor, and disruption of the gene resulted in reduced growth rate, inability to sporulate, increased sensitivity to abiotic stresses, and abolishment of virulence (Lv et al. 2016). *UvSUN2* encodes a SUN domain-containing protein, and mutation in *UvSUN2* led to altered cell wall construction, abnormal fungal growth and stress responses, as well as inability to infect rice (Yu et al. 2015). On the contrary, knock-out or knock-down of *Uvt3277*, a gene encoding a putative low-affinity iron transporter, enhanced *U. virens* virulence (Zheng et al. 2017). Moreover, decoding the *U. virens* genome opens the door for investigation of effectors involved in *U. virens* pathogenesis (Zhang et al. 2014).

Effectors of a pathogenic microbe have versatile roles in manipulating host immunity to promote infection of the pathogen. They act either in interfering with phytohormone and secretory pathways, suppressing the pattern recognition receptor-mediated surveillance system, targeting plasma membrane components and chloroplasts, or generating a microenvironment favorable to infection (Deslandes and Rivas 2012; Dou and Zhou 2012; Kazan and Lyons 2014; Presti et al. 2015). For example, *Phytophthora sojae* effector PsAvr3c can reprogram soybean pre-mRNA splicing system to defeat host immunity and promote infection (Huang et al. 2017). *Pseudomonas syringae* pv. *tomato* injects effectors HopM1 and AvrE1 into Arabidopsis leaves to establish an aqueous space for successful infection (Xin et al. 2016). *P. sojae* secretes a paralogous decoy PsXLP1 to bind host GmGIP1, thus releasing the apoplastic effector PsXEG1 to promote infection (Ma et al. 2017). *U. virens* genome encodes at least 193 putative effector proteins (Zhang et al. 2014). Thirteen of them can induce cell death and 18 can suppress plant hypersensitive responses in *Nicotiana benthamiana* or rice protoplast (Zhang et al. 2014; Fang et al. 2016). However, up to date, none of them has been in-depth investigated during *U. virens* infection.

In an earlier de novo transcriptome analysis (Fan et al. 2015), we detected a full-length candidate effector gene *Uv2169* whose transcription was significantly up-regulated upon *U. virens* infection. *Uv2169* was coincidently reported as *UV_1261* that can suppress *Burkholderia glumae*-induced cell death in *N. benthamiana* (Zhang et al. 2014). Thereafter, we renamed *Uv2169* as *UV_1261*. Here, we examined its expression pattern during infection and tested the effects of knock-down or overexpression of *UV_1261*. The results demonstrated that *UV_1261* specifically suppressed plant defense responses in rice spikelets to facilitate colonization of *U. virens*.

Results

The expression pattern of UV_1261 over *U. virens* infection of rice panicles

To understand how *UV_1261* facilitates *U. virens* infection, we examined its expression pattern during *U. virens* infection by a time-course analysis. To this end, we exploited a compatible *U. virens*-rice interaction established in our previous studies with the isolate PJ52 and the rice accession Pujiang 6 (Fan et al. 2015; Huang et al. 2016). Sequence analysis showed that *UV_1261* in PJ52 was identical to that in the published UV-8b genome (Additional file 1: Figure S1) (Zhang et al. 2014). Compared to its expression in PSB medium, *UV_1261* was up-regulated at 1–3 days post inoculation (dpi), and then slightly decreased from 5 to 9 dpi. It was up-regulated again at 11 dpi, and reached to the highest expression at 13 dpi, forming a bimodal pattern (Fig. 1). This bimodal pattern is coincident with the two infection stages of *U. virens* (Fan et al. 2016), during which no obvious symptoms were detected from 1 to 7 dpi; whereas white fungal mass were seen in inner space of a spikelet at 9 dpi and the fungal mass increased to protrude out of the spikelet at 15 dpi (Fan et al. 2015). Therefore, the expression pattern of *UV_1261* suggested its role in both infection stages.

To check whether *UV_1261* expression was associated with rice defense response, we examined the expression patterns of some defense-related genes, including *OsNAC4*, *OsPR1#012*, *OsPR10b*, and *OsBETV1* (Li et al. 2014b; Fan et al. 2015) over the infection of PJ52 by RT-qPCR. Intriguingly, *OsNAC4* showed an expression pattern reverse to that of *UV_1261* (Fig. 1). Particularly, *OsNAC4* was in low expression at 1, 3, 11 and 13 dpi, when *UV_1261* was highly expressed; whereas, *OsNAC4* was greatly induced from 5 to 9 dpi, when *UV_1261* was at lower expression. *OsPR1#012* and *OsPR10b* were induced at early time points, but down-regulated at later time points, especially at 13 dpi when *UV_1261* reached the highest expression (Fig. 1). By contrast, *OsBETV1* was up-regulated across the infection process, although to a lesser extent at later time points (Fig. 1). These results imply that rice defense response is induced at earlier time points but then suppressed by infection of *U. virens*.

UV_1261 encodes a small secreted cysteine-rich protein

UV_1261 contains a 393 bp codon, encoding a small cysteine-rich protein with 130 amino acid (aa) residues (Fig. 2a). The first 23 aa residues was a predicted signal peptide. First, we verified the function of the predicted signal peptide via an invertase secretion assay following previous studies (Klein et al. 1996; Jacobs et al. 1997; Oh et al. 2009; Cheng et al. 2017). To this end, we cloned the sequence encoding the first 23 aa residues of UV_1261 to the N-terminus of the mature yeast invertase gene *SUC2*

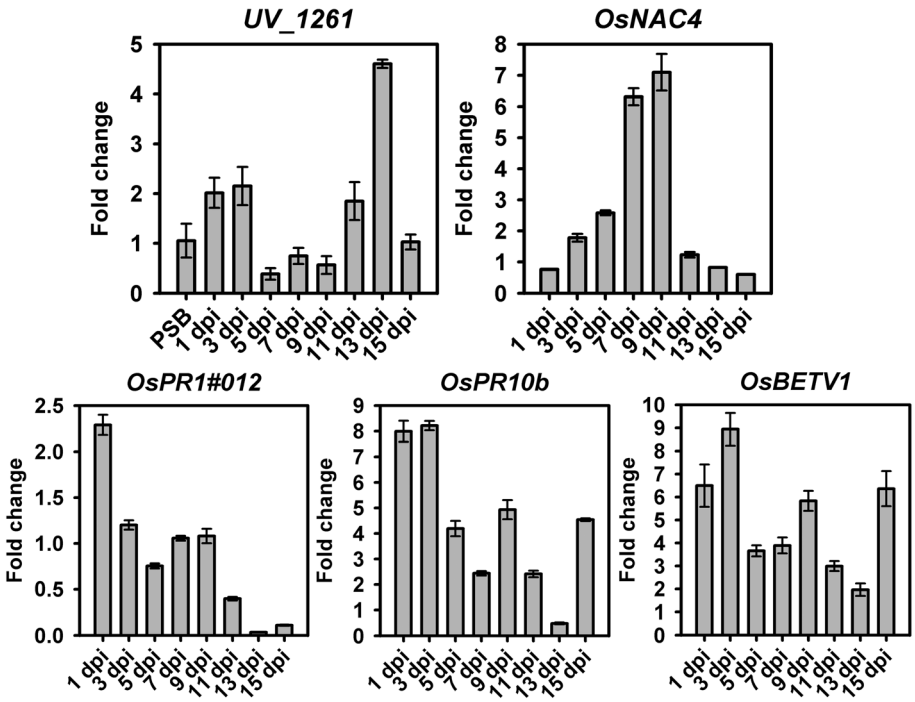

Fig. 1 Expression patterns of *UV_1261* and rice defense-related genes. Total RNAs were prepared from samples collected from 7-day-old PSB-cultured PJ52, and PJ52- or mock-inoculated rice spikelets at indicated time points. RT-qPCR was performed for expression profiling of *UV_1261*, *OsNAC4*, *OsPR1#012*, *OsPR10b* and *OsBETV1*. *UvTub2a* or *OsUbi* was used as the reference gene for *U. virens* or rice gene quantification, respectively. Fold change was calculated by the comparative C_T method $2^{-\Delta\Delta CT}$ using PSB-cultured PJ52 as the control for *UV_1261*, and using mock-inoculated sample at each time point as the control for rice defense-related genes. Error bars indicate standard deviations ($n = 3$)

and transformed into YTK12, a *SUC2*-deficient yeast strain. Similarly, we made constructs with the sequences encoding the first 25 aa residues of *Magnaporthe oryzae* Mg87 and the validated signal peptide of *P. sojae* effector Avr1b as negative and positive control, respectively (Gu et al. 2011; Cheng et al. 2017). Then, the constructs were transformed into YTK12 for invertase secretion assay. As expected, all the three constructs could enable growth of YTK12 on CMD-W medium where yeast can grow without invertase secretion. However, only the constructs expressing SUC2 fused with the signal peptide of UV_1261 and Avr1b could enable YTK12 growth on YPRAA medium where yeast grow requires signal peptide-mediated secretion of the invertase (Fig. 2b). The negative control peptide of Mg87 could not enable YTK12 growth on YPRAA medium. These data indicate that the predicted signal peptide of UV_1261 is functional in mediating secretion.

UV_1261 is mainly localized in the cytoplasm and the chloroplast

To determine the subcellular localization of UV_1261 *in planta*, we cloned the sequence encoding mature UV_1261 (without signal peptide) at the N-terminus of eYFP for transient expression in *N. benthamiana* and stable expression in transgenic Arabidopsis Col-gl. Transient expression showed that UV_1261-eYFP was localized in the cytoplasm, the nucleus and the chloroplasts of *N. benthamiana* cells (Additional file 2: Figure S2a-c). In transgenic Arabidopsis plants, UV_1261-eYFP was mainly aggregated as dots, in addition to scattered distribution in the cytoplasm (Fig. 2c). Intriguingly, the fluorescent signal of UV_1261-eYFP was overlapped with the auto-fluorescent signal of the chloroplasts, indicating localization of UV_1261 in the chloroplasts (Fig. 2d). Moreover, UV_1261-eYFP fusion protein was intact as confirmed by Western blot (Fig. 2e). Taken together, these data indicate that UV_1261-eYFP is localized in the cytoplasm and the chloroplasts.

UV_1261 suppresses basal defense responses in *N. benthamiana* and Arabidopsis

PAMPs like flg22 can trigger basal defense responses, such as rapid burst of ROS, callose deposition and expression of defense-related genes. Thus, we tested whether *UV_1261* played a role in suppression of flg22-triggered defense responses. When *UV_1261* was transiently expressed in *N. benthamiana*, flg22-triggered ROS burst was obviously inhibited (Additional file 2: Figure S2d). When *UV_1261* was stably expressed in Arabidopsis, flg22-induced ROS accumulation was also inhibited (Fig. 3a). Meanwhile, flg22-induced callose deposition was

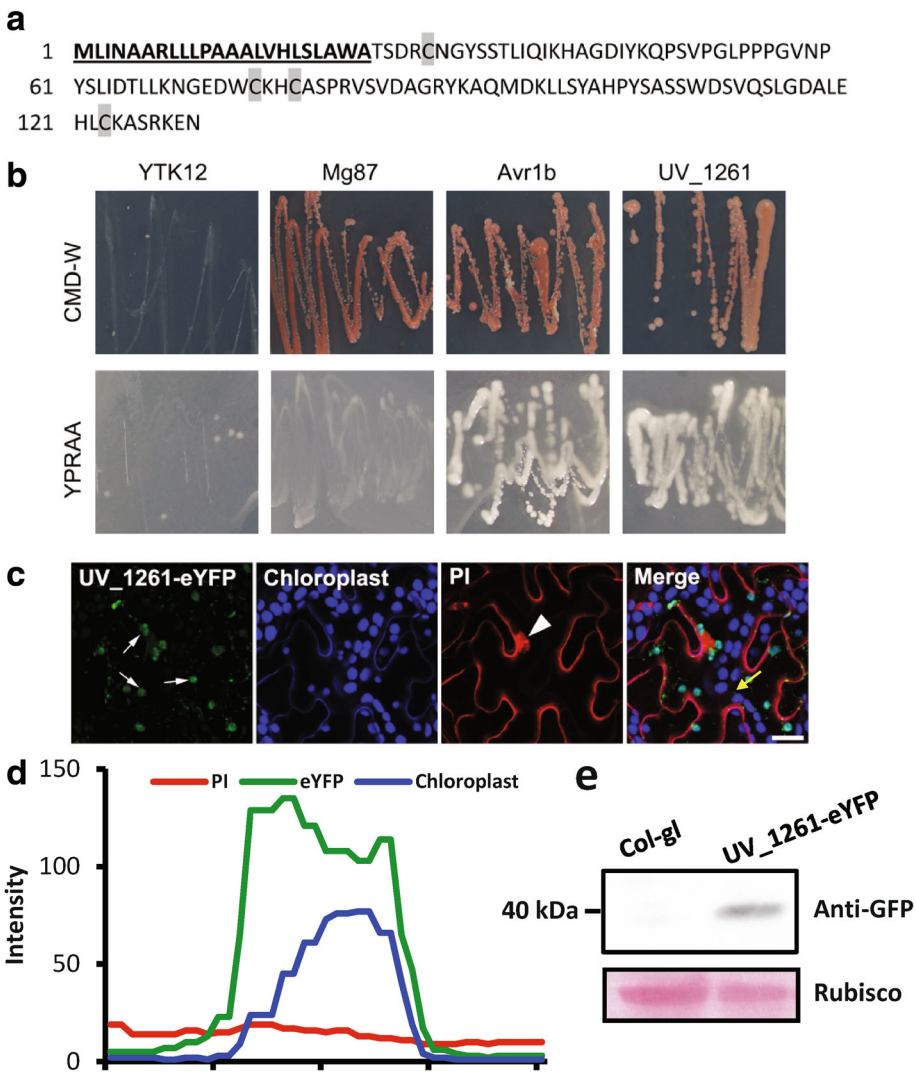

Fig. 2 Signal peptide validation and subcellular localization of UV_1261. **a** Protein sequence of UV_1261. Bold and underlined letters represent putative signal peptide. Shaded letters indicate cysteine residues. **b** Validation of UV_1261 signal peptide by yeast invertase secretion assay. Predicted signal peptide sequence of UV_1261 was fused in-frame to yeast mature invertase sequence in pSUC2 vector and expressed in YTK12. Functional signal peptide could enable yeast growth on both CMD-W and YPRAA. N-terminal sequence of Mg87 and signal peptide of Avr1b were used as the negative and positive control, respectively. **c** The construct *UV_1261-eYFP* was transformed into Arabidopsis Col-gl. After obtaining T_2 transgenic lines, leaves expressing *UV_1261-eYFP* were checked under a confocal laser scanning microscope. Nuclei were stained by PI and false-colored in red. Chloroplasts showed autofluorescence and was false-colored in blue. White arrows point to chloroplasts, and white triangles point to nuclei. Scale bar, 20 μm. **d** Fluorescence intensity curves were drawn according to the direction of the yellow arrow in (**c**). **e** Western blot with GFP antibody in Arabidopsis leaves expressing *UV_1261-eYFP*. The band at 40 kDa indicates the UV_1261-eYFP fusion protein

remarkably reduced in *UV_1261-eYFP* transgenic line (Fig. 3b), being about one-third of that in the wild-type Col-gl. Next, RT-qPCR was performed to examine the expression of defense-related genes in Arabidopsis (Li et al. 2018), including *FLG22-INDUCED RECEPTORLIKE KINASE 1* (*FRK1*, At2g19190), *WRKY29* (At2g23550) and the *PATHOGENESIS-RELATED1* (*PR1*, At2g19990). The expression of *FRK1* and *WRKY29* was highly induced as early as 3 hours post application (hpa) of flg22 in Col-gl, while *PR1* was induced and reached to the highest expression at 12 hpa (Fig. 3c). By contrast, the induction of all the three tested genes were much lower in *UV_1261-eYFP* transgenic line than in Col-gl (Fig. 3c). Taken together, *UV_1261* could suppress basal defense responses in *N. benthamiana* and Arabidopsis.

UV_1261 increases infection of tobacco powdery mildew in Arabidopsis

Modulation of basal defense responses by *UV_1261* prompted us to test whether it can compromise disease

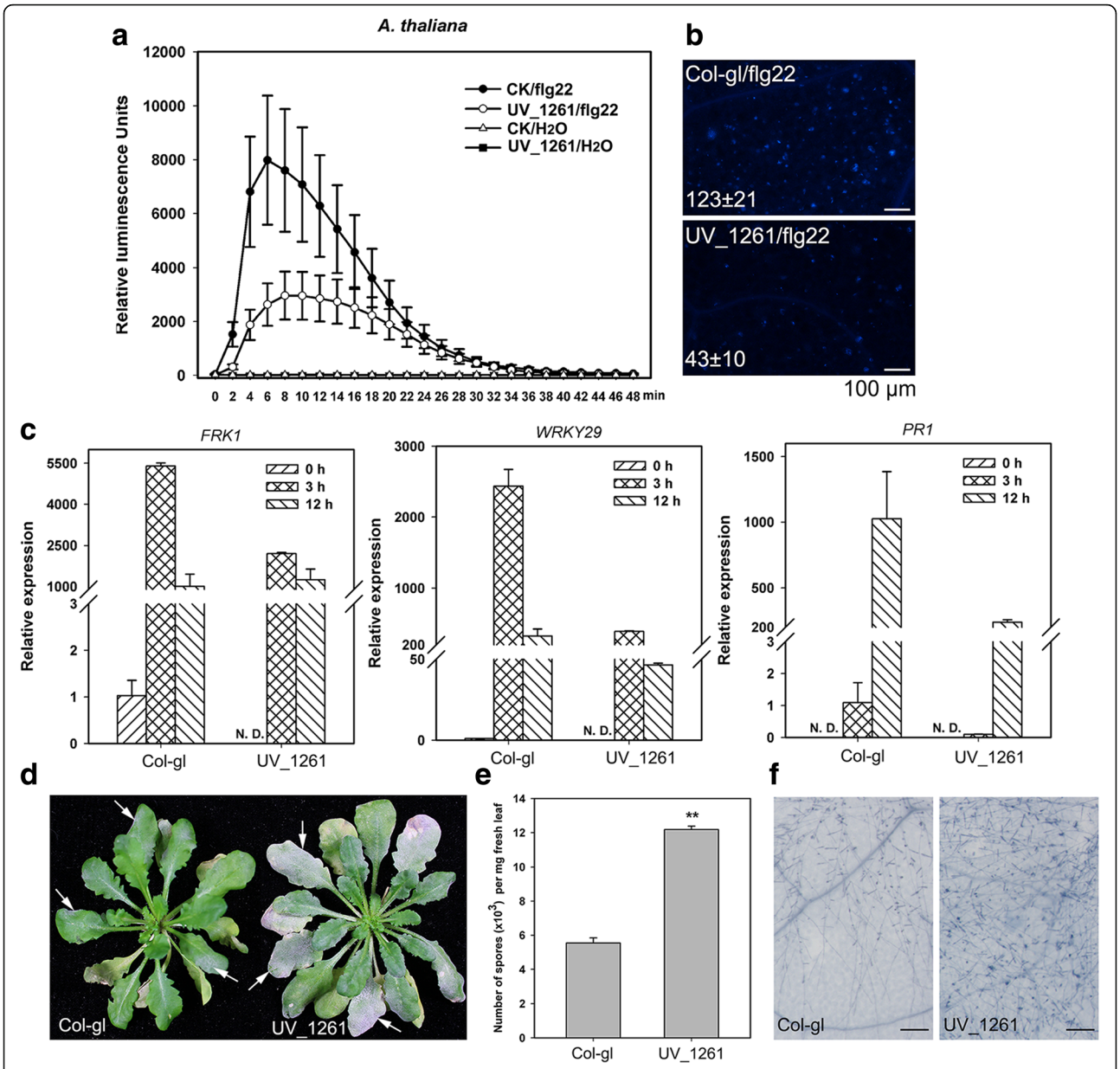

Fig. 3 UV_1261 suppresses plant basal defense responses and promotes powdery mildew infection in Arabidopsis. **a** Flg22-induced ROS burst in Arabidopsis leaves stably expressing *UV_1261-eYFP* or wild-type Col-gl leaves (CK). **b** Comparison of flg22-induced callose deposition in leaves of *UV_1261-eYFP* transgenic plants and Col-gl. **c** Expression profiling of indicated defense-related genes in *UV_1261-eYFP*-expressing Arabidopsis and Col-gl treated with flg22. *AtACT2* was used as a reference gene. Relative expression was normalized to that in Col-gl at 0 h, and calculated by the comparative C_T method $2^{-\Delta\Delta CT}$. N. D., not detected. Error bars indicate standard deviations ($n = 3$). **d** Disease symptom of Col-gl and *UV_1261-eYFP*-expressing Arabidopsis inoculated with powdery mildew isolate *Golovinomyces cichoracearum* SICAU1. White fungal mass was observed on leaf surface (indicated by white arrows). **e** Quantification of powdery mildew spores on leaves of indicated plants. Significant difference was determined by the Student's t-test. **, $P < 0.01$. **f** Trypan blue staining of infected leaves from Col-gl and *UV_1261-eYFP*-expressing Arabidopsis. Much more mycelia were seen on *UV_1261*-expressing leaves than on Col-gl leaves

resistance against biotrophic pathogen. To this end, we inoculated the tobacco powdery mildew strain *Golovinomyces cichoracearum* SICAU1 onto six-week-old plants of *UV_1261-eYFP* transgenic line and Col-gl. The results showed that *UV_1261-eYFP* leaves sustained more white fungal mass and spores than Col-gl leaves at 12 dpi (Fig. 3d, e). Trypan blue staining displayed that there were more hyphae in *UV_1261-eYFP* than in Col-gl leaves (Fig. 3f). These data indicate that *UV_1261* promotes the powdery mildew infection in Arabidopsis.

Exogenous double-stranded siRNA of *UV_1261* reduces *U. virens* virulence

Since exogenous application of double-stranded RNAs can trigger gene silencing (Fire et al. 1998), we employed this approach to preliminarily test whether *UV_1261* was involved in *U. virens* virulence. To this end, we synthesized a 21 bp double-stranded siRNA specifically targeting *UV_1261* and prepared inocula using the strain P4 cultured on media containing 10 nM/mL of the synthesized siRNA. As expected, in the inocula from the siRNA-containing media, the expression of *UV_1261* was reduced to as low as 50% of that in control (Fig. 4a), indicating that the siRNA is functional in silencing of *UV_1261*. Then the inocula were injected into more than 30 rice panicles at late booting stage in comparison with control inocula. After 28 dpi, the number of false smut balls was counted (Fig. 4b). Typically, the number of false smut balls per inoculated panicle varied from less than 10 to more than 50 (Fig. 4b). This is a common phenomenon to rice false smut disease that makes disease assay difficult. To evaluate the effects of different inocula, we classified the diseased panicles into five types according to the number of RFS balls per panicle, i.e. 1–10, 11–20, 21–40, 41–50 and > 50. The data demonstrated that nearly half (47%) of the diseased panicles showed mild infection with the number less than 10 in siRNA-treated group, but less than one third (31%) in control group (Fig. 4c). On the contrary, the percentage of severely diseased panicles (> 20 balls per panicle) was much lower in siRNA-treated group than in control (Fig. 4c). These data indicate that suppression of *UV_1261* in vitro could reduce *U. virens* virulence.

Silencing of *UV_1261* attenuates *U. virens* virulence

To further confirm the role of *UV_1261* in *U. virens* virulence, we tried to knockout *UV_1261* by using gene replacement strategy, but failed to obtain any knockout mutants probably due to low homologous recombination

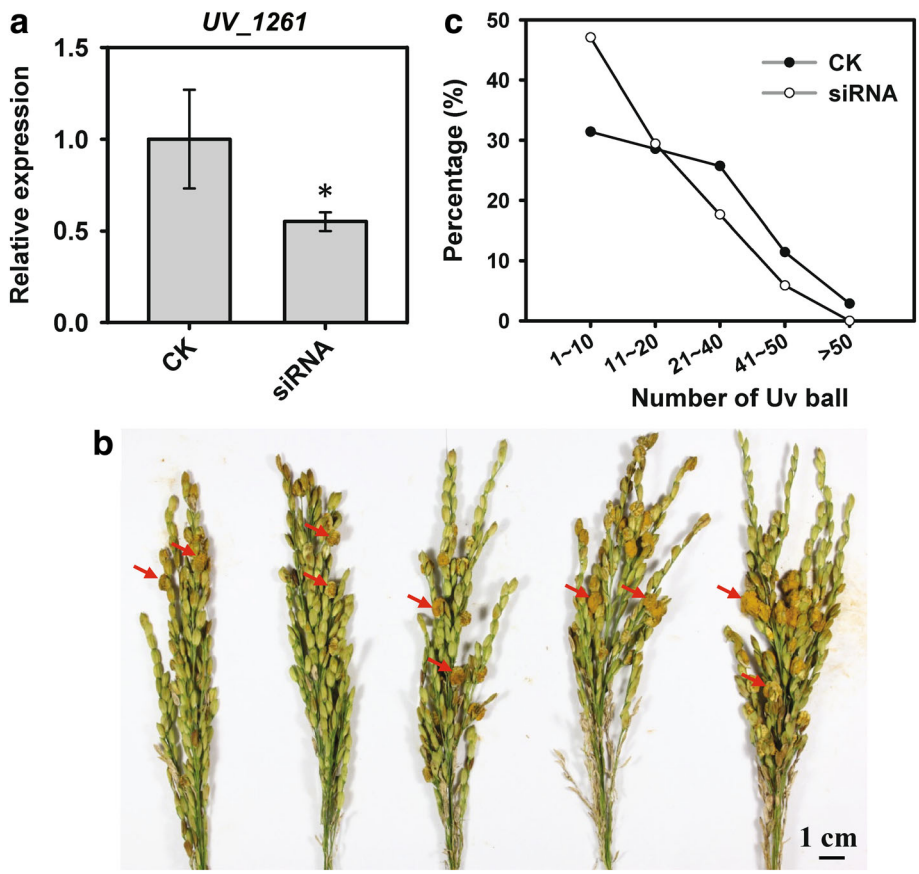

Fig. 4 In vitro application of double-stranded siRNA of *UV_1261* to *U. virens* P4. **a** Double-stranded siRNA specifically targeting UV_1261 was synthesized in vitro and added in PSB culturing *U. virens* isolate P4. Relative expression of *UV_1261* was determined by RT-qPCR using *UvTub2a* as a reference gene. Significant difference was determined by the Student's t-test. **, $P < 0.05$. **b** Representative image of P4-infected rice panicles with variable number of false smut balls. **c** The number of false smut balls in P4-infected rice panicles. P4 inocula were pre-treated with 10 nM double-stranded siRNA of *UV_1261*, and adding with DEPC-treated ddH_2O was set as control (CK). Arrows indicate false smut balls. Uv, *U. virens*

frequency in *U. virens* (Zheng et al. 2016). We then tried to silence *UV_1261* in *U. virens* isolate PJ52. Fortunately, we obtained positive transformants with reduction of *UV_1261* expression. Subsequently, three independent transformants (T1, T2 and T3) with significantly lower expression of *UV_1261* were selected for further analysis (Fig. 5a). All the three transformants formed colonies with diameters similar to that of the wild-type PJ52 after cultured for 2 weeks on PSA, and produced conidia with unaltered morphology (Fig. 5b). To test their virulence, the transformants were inoculated into rice panicles of cultivar Pujiang 6 that is highly susceptible to *U. virens* (Huang et al. 2016). Then, the number of RFS balls in each diseased panicle was recorded at 4 weeks post inoculation (wpi). The results showed that PJ52 and the three transformants all successfully infected rice panicles, with the rate of diseased panicle reaching 100%. PJ52 formed more than 110 RFS balls in average in the inoculated panicles (Fig. 5c). However, the three transformants formed much less number of RFS balls than PJ52 (Fig. 5c, d). In addition, we observed that the expression of *UV_1261* positively correlated with the virulence of *U. virens* (Fig. 5). Therefore, these data confirmed that *UV_1261* is a virulence effector of *U. virens*.

Silencing of *UV_1261* leads to higher expression of rice defense-related genes in *U. virens*-inoculated spikelets

To test whether knockdown of *UV_1261* influenced the induction of rice defense, we inoculated *UV_1261*-silenced transformants (T1 and T3) into rice panicles at booting stage with PJ52 as control, and examined the expressions of four rice defense-related genes at 5 and 9 dpi. Our data showed that the expression of *OsNAC4* remained unchanged at 5 dpi, but was significantly higher in T1 and T3-inoculated spikelets than in PJ52-inoculated control at 9 dpi (Fig. 6). The expression of

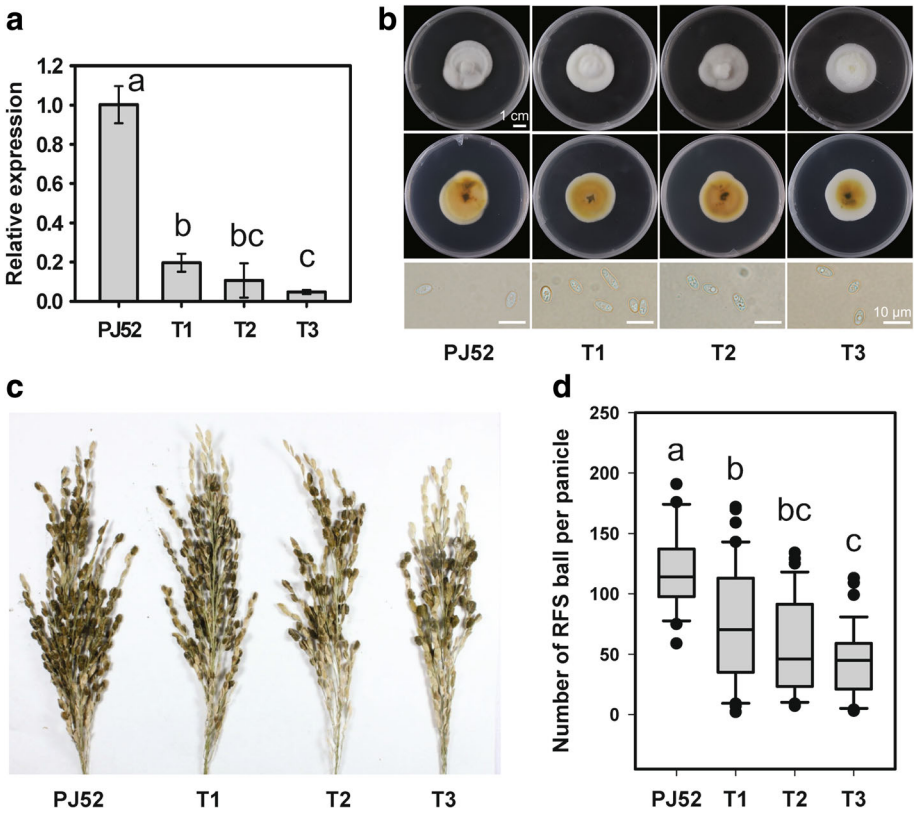

Fig. 5 Phenotype and virulence of *UV_1261*-silenced *U. virens* transformants. **a** Expression level of *UV_1261* in wild-type PJ52 and three transformants. Gene silencing was confirmed by RT-qPCR using *UvTub2a* as a reference gene. PJ52 was set as the control. **b** Representative images of indicated *U. virens* colonies cultured in PSA for 2 weeks, and conidia cultured in PSB for 7 days. Upper panel, top view of colonies from wild-type PJ52 and three transformants T1, T2, T3. Scale bar, 1 cm. Middle panel, bottom view of colonies from wild-type PJ52 and three transformants T1, T2, T3. Lower panel, morphology of conidia from wild-type PJ52 and three transformants T1, T2, T3. Scale bar, 10 μm. **c** Disease assay of wild-type PJ52 and three transformants T1, T2, T3. Each *U. virens* inocula were artificially injected into 30–50 panicles of Pujiang 6 at late booting stage. Representative images of diseased rice panicles infected with PJ52, T1, T2, or T3 were shown. **d** Around 4 wpi, the number of rice false smut ball per panicle was recorded. Statistical analysis was performed with LSD method in SPSS Version 21. Different letters above the data box indicate significant differences at $P < 0.05$

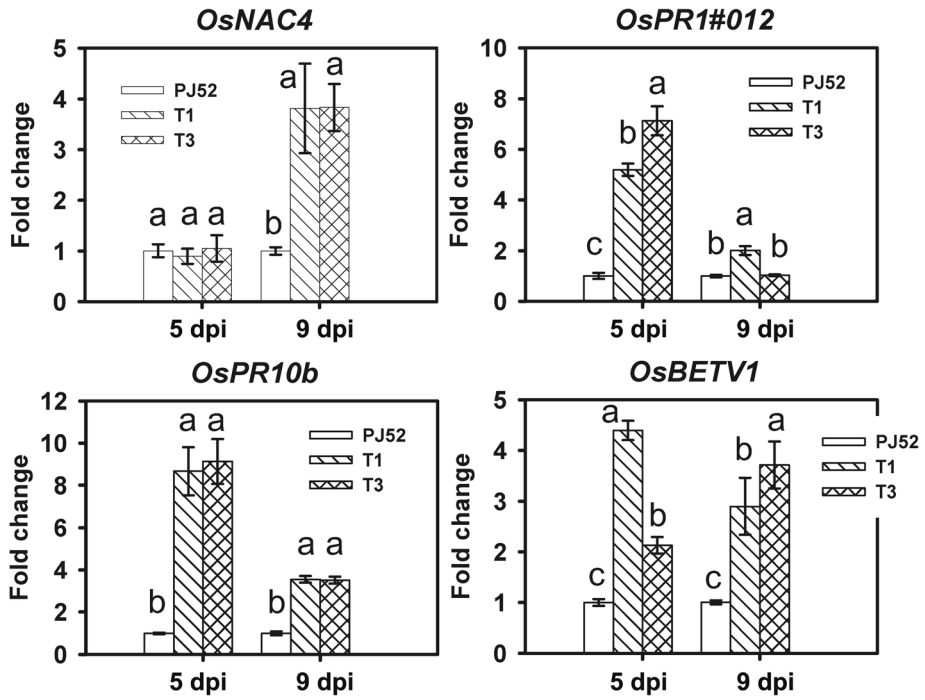

Fig. 6 Expression analysis of rice defense-related genes in response to infection of PJ52 and *UV_1261*-silenced transformants. Rice spikelet samples inoculated with PJ52, T1, or T3 were collected at 5 and 9 dpi. Expression levels of *OsNAC4*, *OsPR1#012*, *OsPR10b*, and *OsBETV1* were determined by RT-qPCR using rice *OsUbi* as the reference gene. Fold change was calculated by the comparative C_T method $2^{-\Delta\Delta CT}$ using PJ52-inoculated samples as controls at indicated time points. Statistical analysis was performed with LSD method in SPSS Version 21. Different letters above the bars mean significant differences among datasets at each indicated time point ($P < 0.05$)

OsPR10b at 5 dpi was increased to about 9-fold in T1 or T3-inoculated spikelets compared with that in control, and nearly 4-fold at 9 dpi (Fig. 6). Similar trend was shown for *OsPR1#012*. The expression of *OsBETV1* was increased to 2–4 fold in T1 or T3-inoculated spikelets at both 5 and 9 dpi. Overall, compared to PJ52-inoculated spikelets, T1 and T3-inoculated samples exhibited significantly higher expression of all four tested genes at either 5 and/or 9 dpi, indicating that *UV_1261*-silenced strains cannot efficiently suppress the expression of rice defense-related genes. Therefore, these data implied that *UV_1261* promotes *U. virens* infection via suppression of host defense.

UV_1261 has no intra-species diversity

BLAST analysis showed that *UV_1261* had no homologs in *U. virens* genome and no orthologs in any other published fungal genomes, indicating that *UV_1261* is a single gene specific in *U. virens*. Then, evolutionary analysis was performed on 50 *U. virens* isolates collected from different rice production areas in China (Additional file 3: Table S1). The results showed that these *U. virens* isolates were classified into five subgroups, and isolates from different locations could be grouped together (Additional file 4: Figure S3a). These isolates were used to amplify the full-length of *UV_1261*. Sequence analysis revealed that *UV_1261* sequences from all the tested isolates were identical (Additional file 4: Figure S3b), suggesting that *UV_1261* is extremely conserved among *U. virens* isolates.

Discussion

There are 193 putative effectors in *U. virens* genome (Zhang et al. 2014), none of them was reported to be involved in *U. virens* pathogenicity. In this study, we demonstrated that *UV_1261* is a *U. virens*-specific effector involved in suppressing plant defense responses and required for full virulence of *U. virens*.

Fungal effectors are featured by low sequence similarity and lack of conserved motif within and across species (Sperschneider et al. 2015), although some exceptions exist, such as the LysM domain-containing effectors Ecp6 from *Cladosporium fulvum* and Slp1 from *M. oryzae* (de Jonge et al. 2010; Mentlak et al. 2012). In addition, fungal effectors are also defined to be secreted from the pathogen and their expression should be induced *in planta* during pathogenesis (Guyon et al. 2014; Sperschneider et al. 2014). In consistent with these criteria for defining an effector, UV_1261 is a *U. virens*-specific effector. First, no homologous sequence of *UV_1261* was found in *U. virens*

or other fungal genomes. Second, Interpro search revealed no conserved domain in UV_1261 protein. Third, UV_1261 possessed a functional signal peptide at its N-terminus (Fig. 2b), and expression of *UV_1261* was significantly induced in *U. virens* upon infection of rice (Fig. 1).

Knock-out or knock-down a single effector usually does not affect virulence, due to functional redundancy of the effector pool in a pathogen genome (Birch et al. 2008). For instance, silencing of *PSTha5a23* in *Puccinia striiformis* f. sp. *tritici* did not change its virulence in wheat (Cheng et al. 2017). Knock-out *AvrPi9* or other 77 putative effector genes in *M. oryzae* also did not affect its virulence in rice (Saitoh et al. 2012; Wu et al. 2015). However, deletion of core effectors may compromise the virulence of pathogens. For example, disruption of the core effector *pep1* in *Ustilago maydis* caused inability of the pathogen to infect maize leaf, although the *Δpep1* mutants had normal saprophytic growth (Doehlemann et al. 2009). In this study, silencing of *UV_1261* in vitro and in vivo consistently showed reduction of *U. virens* virulence, indicating that *UV_1261* is a core effector (Fig. 4 and Fig. 5).

In addition to photosynthesis and primary metabolism, chloroplast is involved in production of pro-defense molecules, such as SA, JA, ABA, ROS and calcium (Serrano et al. 2016). Pathogens have evolved effectors to interfere with chloroplast function, so as to fight against host immunity. For instance, *P. syringae* pv. *tomato* secretes a effector protein HopN1 to interact with PsbQ in thylakoids, resulting in reduction of chloroplastic ROS (Rodriguez-Herva et al. 2012). *Pst* effectors HopK1 and AvrRps4 also target to host chloroplasts to suppress ROS production, although their targeted proteins are unknown (Li et al. 2014a). Effector proteins Cmu1 from *U. maydis* (Djamei et al. 2011), PsIsc1 from *P. sojae* and VdIsc1 from *Verticillium dahliae* (Liu et al. 2014) modulate SA biosynthesis in plastid and suppress plant immune responses. In the present work, UV_1261 was targeted to chloroplasts (Fig. 2c-e), suggesting its role in interfering with plant immunity, which was further supported by that UV_1261 could suppress basal defenses in *N. benthamiana*, Arabidopsis and rice (Fig. 3, Fig. 6 and Additional file 2: Figure S2d).

Pathogen effectors are subjected to rapid evolution, so as to evade the recognition by host resistance proteins. For example, insertion of transposable element and somatic exchange in wheat stem rust effector protein AvrSr35 and AvrSr50, respectively, drove the pathogen escaping recognition by R proteins Sr35 and Sr50 (Chen et al. 2017; Salcedo et al. 2017). Mg-SINE insertion in *M. oryzae AvrPi9* converted an avirulent isolate to a virulent isolate (Wu et al. 2015). However, in our work, no polymorphism was detected in *UV_1261* from around 50 *U. virens* isolates collected across multiple rice production areas in China (Additional file 4: Figure S3), implying that *UV_1261* is of extremely low intraspecific variation.

Conclusions

Overall, UV_1261 is a novel core effector protein that plays an important role in *U. virens* virulence by suppressing plant defense responses. As *UV_1261* is unique and highly conserved in *U. virens*, it could be a potential molecular target for developing efficient strategies to control RFS disease.

Methods

Plant materials and pathogen isolates

Plants of rice cultivar Pujiang 6 were grown in an experimental field under natural conditions. *N. benthamiana* and Arabidopsis accession Col-gl were planted in a growth room at 10 h light/14 h darkness, 23 °C and 70% relative humidity until subsequent experiments. *U. virens* isolates were obtained via amerosporous purification from RFS balls. *U. virens* isolate PJ52 was used for gene expression analysis and *U. virens* transformation experiments. The GFP-tagged *U. virens* strain P4 was used for siRNA treating experiment. The powdery mildew *Golovinomyces cichoracearum* SICAU1 (Zhang et al. 2015) was maintained on leaves of tobacco in a growth room at 16 h light/8 h darkness, 23 °C and 75% relative humidity.

U. virens inoculation

Artificial inoculation of *U. virens* was performed as described previously (Fan et al. 2015). In brief, *U. virens* mycelia were cultured in potato-sucrose broth (PSB) at 28 °C and 120 r/min for 5–7 days, and the mixture of mycelia and conidia were blended as inocula, with conidia concentration adjusted to 1×10^6 conidia/mL. At late booting stage of rice (5–7 days before heading), *U. virens* inocula were injected into rice panicles by a syringe with needle. Mock-inoculation was carried out with PSB. Rice spikelets were collected at 1, 3, 5, 7, 9, 11, 13 and 15 dpi for subsequent experiments. The number of false smut balls was recorded at about 4 wpi.

Quantitative RT-PCR

Total RNA was extracted using TRIzol reagent (Invitrogen) and was reverse transcribed using SuperScriptfirst-strand synthesis kit (Invitrogen). Quantitative RT-PCR (RT-qPCR) was performed using SYBR Green mix (TaKaRa) and gene specific primers (Additional file 5: Table S2). The reference gene *UvTub2α* was used for expression analysis of *UV_1261*, *OsUbi* for rice genes, and *AtACT2* for Arabidopsis genes. Comparative C_T method $2^{-\Delta\Delta CT}$ (Livak and Schmittgen 2001) was applied for calculating relative expression.

Plasmid construction

For validation of UV_1261 signal peptide, the corresponding DNA fragment was amplified with primer pair SP1261_EcoRIF/SP1261_XhoIR, and inserted into pSUC2T7M13ORI (pSUC2) vector at restriction enzyme sites *Eco*RI and *Xho*I. For ectopic expression of *UV_1261* in *N. benthamiana* and Arabidopsis, primer pair Uvm1261_KpnIF/Uv1261_KpnIR was used to amplify the full-length of *UV_1261* minus signal peptide sequence, and inserted into pCAMBIA1300-eYFP vector with *Kpn*I. For *U. virens* transformation, 1261_EcoRIF/1261_SpeIR were used to amplify the antisense strand of *UV_1261*, and inserted into Pzp-bar-Ex vector (Additional file 6: Figure S4) to silence *UV_1261*.

Yeast invertase secretion assay

pSUC2-derived plasmids were transformed into yeast strain YTK12 with the lithium acetate method (Gietz et al. 1995). The subsequent procedures of yeast secretion assay was performed as described (Fang et al. 2016).

Agrobacterium tumefaciens-mediated transformation

A. tumefaciens strain GV3101 containing *UV_1261-eYFP* construct was transiently expressed in *N. benthamiana* as described (Huang et al. 2014) and stably expressed in Arabidopsis Col-gl with floral dipping method (Clough and Bent 1998). *A. tumefaciens* strain AGL1 containing *UV_1261*-related constructs were transformed into conidia of PJ52 according to the published protocol with modifications (Yu et al. 2015). In brief, PJ52 conidia were produced in PSB medium at 28 °C, 120 r/min for 7 days. AGL1 containing indicated constucts was cultured in minimal medium at 28 °C, 200 r/min for 48 h, supplemented with 50 μg/mL kanamycin. Then diluted AGL1 (OD600 = 0.15) was pre-cultured in induction medium, supplemented with 50 μg/mL kanamycin and 50 μM acetosyringone, for about 6 h until OD600 reaching 0.25. One hundred microliter of AGL1 cells were mixed with equal volume of 10^6 conidia/mL PJ52, and incubated on nitrocellulose membrane (Whatman, pore size = 0.45 μm) in co-cultivation medium at 25–28 °C for 72 h. The membrane was then transferred to the selection medium, i.e. potato-sucrose-agar (PSA) medium with 0.003% Basta (Yobios BioTect) and 500 μg/mL Timentin (Solarbio), and incubated at 25–28 °C until transformants appeared. The colonies were again transferred to selection medium to screen for positive transformants, which were further confirmed by PCR with primer pairs UvmitoF/UvmitoR, BastaF/BastaR, and 1261_EcoRIF/TtrpC_R. *UV_1261* expression were examined by RT-qPCR with the primer pair UV_1261_F2 /UV_1261_R2. Primer sequences are included in Additional file 5: Table S2.

Subcellular localization

The construct *UV_1261-eYFP* or empty vector expressing only eYFP was co-expressed with *2 × RFP-NLS* (Huang et al. 2014) in *N. benthamiana*. Leaves were sampled at 3 days post infiltration for microscopy observation. Fully expanded leaves from T_2 generation of transgenic Arabidopsis (5–6 week old) expressing *UV_1261-eYFP* were sampled and stained in Propidium Iodide (PI) for 10 min before observation. Leaf samples were checked under a confocal laser scanning microscope (Nikon A1). The image data were processed with NIS-Elements viewer and Adobe Photoshop. Western blot was performed with anti-GFP sera (BBI Life Science).

ROS, callose assays and trypan blue staining

Leaves of Col-gl and *UV_1261-eYFP*-expressing plants were prepared and treated with either ddH_2O or 1 μM flg22, and subjected to ROS and callose assays as previously described (Li et al. 2018). Spores of powdery mildew SICAU1 were inoculated onto leaves of Col-gl and transgenic line expressing *UV_1261-eYFP*. Spore production was determined and pathogen hyphae were stained with trypan blue according to the reported method (Zhao et al. 2015). Images were acquired under a Canon EOS Rebel T2i.

siRNA treatment

Double-stranded siRNA specifically targeting *UV_1261* was designed and synthesized by Shanghai GenePharma Co., Ltd. The sequences are listed in Additional file 5: Table S2. SiRNA was dissolved in DEPC-treated ddH_2O and added in PSB to a final concentration of 10 nM. *U. virens* inocula were prepared from 7-day-old PSB-cultured P4, and 10 nM siRNA was added again in inocula before artificial inoculation. The control group was added with DEPC-treated ddH_2O.

DNA polymorphism analysis

Primer pair Uv1261_SNPF/Uv1261_SNPR was used for amplifying the full-length DNA of *UV_1261*. To identify the evolutionary relationships among the examined *U. virens* isolates, primer pair UvSNP1_F/UvSNP1_R was used for amplifying a SNP-rich region in *U. virens* genome (Sun et al. 2013), and the obtained sequences were subjected to evolutionary analysis in MEGA5 using the Neighbor-Joining method with default parameters (Tamura et al. 2011). Primers are presented in Additional file 5: Table S2.

Sequence analysis and data processing

BLAST analysis was conducted at NCBI online (http://blast.ncbi.nlm.nih.gov/). Signal peptide prediction of UV_1261 was performed on SignalP 4.0 Server (http://www.cbs.dtu.dk/services/SignalP-4.0/) (Petersen et al. 2011). Sequence alignment was carried out with MultAlin (http://multalin.toulouse.inra.fr/multalin/multalin.html) (Corpet

1988). Conserved domain analysis was performed with Interpro search (http://www.ebi.ac.uk/interpro). Excel and SigmaPlot Version 10.0 were used for data processing. SPSS Version 21 was applied for statistical analysis.

Additional files

Additional file 1 : **Figure S1.** Sequence alignment between *PJ52_UV1261* and *UV8b_UV1261*. (TIF 3479 kb)

Additional file 2 : **Figure S2. a** Mature protein sequence of UV_1261 (without signal peptide) was fused to eYFP and transiently expressed in leaves of *N. benthamiana*. Empty vector (EV) expressing only eYFP was set as a control. The construct *2 × RFP-NLS* was co-expressed as a nucleus indicator. Scale bar, 10 μm. **b** Fluorescence intensity curves were drawn according to the direction of the red arrow in **a**. **c** Western blot with GFP antibody in *N. benthamiana* leaves expressing *eYFP* or *UV_1261-eYFP*. The band at 40 kDa indicates the UV_1261-eYFP fusion protein, while the band at 27 kDa presents free eYFP. **d** Flg22-induced ROS burst in *N. benthamiana* leaves transiently expressing *UV_1261-eYFP* or empty vector (CK). (TIF 1569 kb)

Additional file 3 : **Table S1.** *U. virens* isolates used for DNA polymorphism analysis. (XLSX 10 kb)

Additional file 4 : **Figure S3. a** Evolutionary relationships of 48 *U. virens* isolates from different rice production areas. Evolutionary analyses were conducted in MEGA5 using the Neighbor-Joining method with default parameters. The evolutionary distances were calculated using the Maximum Composite Likelihood method. Bootstrap test with 1000 replicates was performed. **b** Sequence alignment of *UV_1261* among 49 *U. virens* isolates revealed that all the examined *UV_1261* sequences were identical. Uv8b is the isolate that has a reference genome (Zhang et al. 2014). Information of other 48 isolates is presented in Additional file 3: Table S1. (TIF 9076 kb)

Additional file 5 : **Table S2.** Primers used in this study. (XLSX 10 kb)

Additional file 6 : **Figure S4.** Schematic diagram of vector Pzp-bar-Ex used for *U. virens* transformation. (TIF 123 kb)

Abbreviations

eYFP: Enhanced yellow fluorescent protein; PAMP: Pathogen-associated molecular pattern; PI: Propidium iodide; PSA: Potato sucrose agar; PSB: Potato sucrose broth; RFS: Rice false smut; ROS: Reactive oxygen species; RT-qPCR: Quantitative reverse transcription-polymerase chain reaction

Acknowledgements

We thank Dr. YF Liu (Jiangsu Academy of Agricultural Sciences) for kindly providing the GFP-tagged *U. virens* isolate P4 and other *U. virens* isolates purified from RFS balls in Jiangsu Province. We thank Drs. DW Hu (Zhejiang University), CX Luo (Huazhong Agricultural University) and CQ Zang (Liaoning Academy of Agricultural Sciences) for providing *U. virens* isolates used for polymorphism analysis. We also thank Dr. WX Sun (China Agricultural University) for the courtesy of yeast strain YTK12 and pSUC2-derived plasmids. We thank Dr. JMJ Jeyakumar (Sichuan Agricultural University) for critical reading of this manuscript.

Funding

National Natural Science Foundation of China (grant no. 31501598 and 31772241) and Key Projects of Sichuan Provincial Education Department.

Availability of data and materials

All data generated or analysed during this study are included in this published article and its supplementary information files.

Authors' contributions

W-MW and JF designed the research and wrote the manuscipt. JF, ND, LL, G-BL, Y-QW, Y-FZ, X-HH, JL performed the research. JF, ND, LL, J-QZ, YL, FH and W-MW analyzed and interpreted the data. All authors read and approved the final manuscript.

Ethics approval and consent to participate

Not applicable.

Consent for publication

Not applicable.

Competing interests

The authors declare that they have no competing interests.

Author details

[1]Rice Research Institute, Sichuan Agricultural University, 211 Huimin Road, Wenjiang District, Chengdu 611130, China. [2]Collaborative Innovation Center for Hybrid Rice in Yangtze River Basin, Sichuan Agricultural University, 211 Huimin Road, Wenjiang District, Chengdu 611130, China. [3]College of Agronomy, Sichuan Agricultural University, Chengdu 611130, China. [4]Institute of Agricultural Ecology, Sichuan Agricultural University, Chengdu 611130, China. [5]Present Address: Clinical Laboratory of BGI Health, BGI-Shenzhen, Shenzhen 518083, China.

Received: 5 November 2018 Accepted: 15 February 2019
Published online: 08 March 2019

References

Ashizawa T, Takahashi M, Arai M, Arie T. Rice false smut pathogen, *Ustilaginoidea virens*, invades through small gap at the apex of a rice spikelet before heading. J Gen Plant Pathol. 2012;78:255–9.

Birch PRJ, Boevink PC, Gilroy EM, Hein I, Pritchard L, Whisson SC. Oomycete RXLR effectors: delivery, functional redundancy and durable disease resistance. Curr Opin Plant Biol. 2008;11:373–9.

Chen JP, Upadhyaya NM, Ortiz D, Sperschneider J, Li F, Bouton C, et al. Loss of AvrSr50 by somatic exchange in stem rust leads to virulence for Sr50 resistance in wheat. Science. 2017;358:1607–10.

Cheng YL, Wu K, Yao JN, Li SM, Wang XJ, Huang LL, et al. PSTha5a23, a candidate effector from the obligate biotrophic pathogen *Puccinia striiformis* f. sp *tritici*, is involved in plant defense suppression and rust pathogenicity. Environ Microbiol. 2017;19:1717–29.

Clough SJ, Bent AF. Floral dip: a simplified method for *Agrobacterium*-mediated transformation of *Arabidopsis thaliana*. Plant J. 1998;16:735–43.

Corpet F. Multiple sequence alignment with hierarchical clustering. Nucleic Acids Res. 1988;16:10881–90.

de Jonge R, Peter van Esse H, Kombrink A, Shinya T, Desaki Y, Bours R, et al. Conserved fungal LysM effector Ecp6 prevents chitin-triggered immunity in plants. Science. 2010;329:953–5.

Deslandes L, Rivas S. Catch me if you can: bacterial effectors and plant targets. Trends Plant Sci. 2012;17:644–55.

Djamei A, Schipper K, Rabe F, Ghosh A, Vincon V, Kahnt J, et al. Metabolic priming by a secreted fungal effector. Nature. 2011;478:395–8.

Doehlemann G, van der Linde K, Amann D, Schwammbach D, Hof A, Mohanty A, et al. Pep1, a secreted effector protein of *Ustilago maydis*, is required for successful invasion of plant cells. PLoS Pathog. 2009;5:e1000290.

Dou DL, Zhou JM. Phytopathogen effectors subverting host immunity: different foes, similar battleground. Cell Host Microbe. 2012;12:484–95.

Fan J, Chen C, Yu Q, Khalaf A, Achor DS, Brlansky RH, et al. Comparative transcriptional and anatomical analyses of tolerant rough lemon and susceptible sweet orange in response to '*Candidatus* Liberibacter asiaticus' infection. Mol Plant-Microbe Interact. 2012;25:1396–407.

Fan J, Guo XY, Li L, Huang F, Sun WX, Li Y, et al. Infection of *Ustilaginoidea virens* intercepts rice seed formation but activates grain-filling-related genes. J Integr Plant Biol. 2015;57:577–90.

Fan J, Yang J, Wang YQ, Li GB, Li Y, Huang F, et al. Current understanding on *Villosiclava virens*, a unique flower-infecting fungus causing rice false smut disease. Mol Plant Pathol. 2016;17:1321–30.

Fang A, Han Y, Zhang N, Zhang M, Liu L, Li S, et al. Identification and characterization of plant cell death-inducing secreted proteins from *Ustilaginoidea virens*. Mol Plant-Microbe Interact. 2016;29:405–16.

Fire A, Xu S, Montgomery MK, Kostas SA, Driver SE, Mello CC. Potent and specific genetic interference by double-stranded RNA in *Caenorhabditis elegans*. Nature. 1998;391:806.

Gietz RD, Schiestl RH, Willems AR, Woods RA. Studies on the transformation of intact yeast cells by the LiAc/SS-DNA/PEG procedure. Yeast. 1995;11:355–60.

Gu BA, Kale SD, Wang QH, Wang DH, Pan QN, Cao H, et al. Rust secreted protein Ps87 is conserved in diverse fungal pathogens and contains a RXLR-like motif sufficient for translocation into plant cells. PLoS One. 2011; 6:e27217.

Guyon K, Balague C, Roby D, Raffaele S. Secretome analysis reveals effector candidates associated with broad host range necrotrophy in the fungal plant pathogen Sclerotinia sclerotiorum. BMC Genomics. 2014;15:336.

Hu M, Luo L, Wang S, Liu Y, Li J. Infection processes of *Ustilaginoidea virens* during artificial inoculation of rice panicles. Eur J Plant Pathol. 2014;139:67–77.

Huang F, Li Y, Shi J, Fan J, Xu Y-J, Wang W-M. Screening and polymorphism analysis of rice germplasms for resistance to false smut disease in Sichuan Province. Acta Phytopathol Sin. 2016;46:247–57 (in Chinese).

Huang J, Gu LF, Zhang Y, Yan TX, Kong GH, Kong L, et al. An oomycete plant pathogen reprograms host pre-mRNA splicing to subvert immunity. Nat Commun. 2017;8:2051.

Huang YY, Shi Y, Lei Y, Li Y, Fan J, Xu YJ, et al. Functional identification of multiple nucleocytoplasmic trafficking signals in the broad-spectrum resistance protein RPW8.2. Planta. 2014;239:455–68.

Jacobs KA, Collinsracie LA, Colbert M, Duckett M, Goldenfleet M, Kelleher K, et al. A genetic selection for isolating cdnas encoding secreted proteins. Gene. 1997;198:289–96.

Kazan K, Lyons R. Intervention of phytohormone pathways by pathogen effectors. Plant Cell. 2014;26:2285–309.

Klein RD, Gu Q, Goddard A, Rosenthal A. Selection for genes encoding secreted proteins and receptors. Proc Natl Acad Sci U S A. 1996;93:7108–13.

Koiso Y, Li Y, Iwasaki S, Hanaoka K, Kobayashi T, Sonoda R, et al. Ustiloxins, antimitotic cyclic peptides from false smut balls on rice panicles caused by *Ustilaginoidea virens*. J Antibiot (Tokyo). 1994;47:765–73.

Li GY, Froehlich JE, Elowsky C, Msanne J, Ostosh AC, Zhang C, et al. Distinct *Pseudomonas* type-III effectors use a cleavable transit peptide to target chloroplasts. Plant J. 2014a;77:310–21.

Li Y, Lu YG, Shi Y, Wu L, Xu YJ, Huang F, et al. Multiple rice microRNAs are involved in immunity against the blast fungus *Magnaporthe oryzae*. Plant Physiol. 2014b;164:1077–92.

Li Y, Zhang Y, Wang QX, Wang TT, Cao XL, Zhao ZX, et al. Resistance to powdery mildew8.1 boosts pattern-triggered immunity against multiple pathogens in Arabidopsis and rice. Plant Biotechnol J. 2018;16:428–41.

Liu T, Song T, Zhang X, Yuan H, Su L, Li W, et al. Unconventionally secreted effectors of two filamentous pathogens target plant salicylate biosynthesis. Nat Commun. 2014;5:4686.

Livak KJ, Schmittgen TD. Analysis of relative gene expression data using real-time quantitative PCR and the 2(T)(−delta delta C) method. Methods. 2001;25:402–8.

Lv B, Zheng L, Liu H, Tang JT, Hsiang T, Huang JB. Use of random T-DNA mutagenesis in identification of gene *UvPRO1*, a regulator of conidiation, stress response, and virulence in *Ustilaginoidea virens*. Front Microbiol. 2016;7:2086.

Ma Z, Zhu L, Song T, Wang Y, Zhang Q, Xia Y, et al. A paralogous decoy protects *Phytophthora sojae* apoplastic effector PsXEG1 from a host inhibitor. Science. 2017;355:710–4.

Mentlak TA, Kombrink A, Shinya T, Ryder LS, Otomo I, Saitoh H, et al. Effector-mediated suppression of chitin-triggered immunity by *Magnaporthe oryzae* is necessary for rice blast disease. Plant Cell. 2012;24:322–5.

Nakamura K, Izumiyama N, Ohtsubo K, Koiso Y, Iwasaki S, Sonoda R, et al. "Lupinosis"-like lesions in mice caused by ustiloxin, produced by *Ustilaginoieda virens*: a morphological study. Nat Toxins. 1994;2:22–8.

Ngugi HK, Scherm H. Biology of flower-infecting fungi. Annu Rev Phytopathol. 2006;44:261–82.

Oh SK, Young C, Lee M, Oliva R, Bozkurt TO, Cano LM, et al. In planta expression screens of *Phytophthora infestans* RXLR effectors reveal diverse phenotypes, including activation of the *Solanum bulbocastanum* disease resistance protein Rpi-blb2. Plant Cell. 2009;21:2928–47.

Petersen TN, Brunak S, Heijne G, Nielsen H. SignalP 4.0: discriminating signal peptides from transmembrane regions. Nat Methods. 2011;8:785–6.

Presti LL, Lanver D, Schweizer G, Tanaka S, Liang L, Tollot M, et al. Fungal effectors and plant susceptibility. Annu Rev Plant Biol. 2015;66:513–45.

Rodriguez-Herva JJ, Gonzalez-Melendi P, Cuartas-Lanza R, Antunez-Lamas M, Rio-Alvarez I, Li Z, et al. A bacterial cysteine protease effector protein interferes with photosynthesis to suppress plant innate immune responses. Cell Microbiol. 2012;14:669–81.

Saitoh H, Fujisawa S, Mitsuoka C, Ito A, Hirabuchi A, Ikeda K, et al. Large-scale gene disruption in *Magnaporthe oryzae* identifies MC69, a secreted protein required for infection by monocot and dicot fungal pathogens. PLoS Pathog. 2012;8(5):e1002711. https://doi.org/10.1371/journal.ppat.1002711.

Salcedo A, Rutter W, Wang SC, Akhunova A, Bolus S, Chao SM, et al. Variation in the AvrSr35 gene determines Sr35 resistance against wheat stem rust race Ug99. Science. 2017;358:1604–6.

Serrano I, Audran C, Rivas S. Chloroplasts at work during plant innate immunity. J Exp Bot. 2016;67:3845–54.

Song JH, Wei W, Lv B, Lin Y, Yin WX, Peng YL, et al. Rice false smut fungus hijacks the rice nutrients supply by blocking and mimicking the fertilization of rice ovary. Environ Microbiol. 2016;18:3840–9.

Sperschneider J, Dodds PN, Gardiner DM, Manners JM, Singh KB, Taylor JM. Advances and challenges in computational prediction of effectors from plant pathogenic fungi. PLoS Pathog. 2015;11:e1004806.

Sperschneider J, Ying H, Dodds PN, Gardiner DM, Upadhyaya NM, Singh KB, et al. Diversifying selection in the wheat stem rust fungus acts predominantly on pathogen-associated gene families and reveals candidate effectors. Front Plant Sci. 2014;5:372.

Sun X, Kang S, Zhang Y, Tan X, Yu Y, He H, et al. Genetic diversity and population structure of rice pathogen *Ustilaginoidea virens* in China. PLoS One. 2013;8: e76879.

Tamura K, Peterson D, Peterson N, Stecher G, Nei M, Kumar S. MEGA5: molecular evolutionary genetics analysis using maximum likelihood, evolutionary distance, and maximum parsimony methods. Mol Biol Evol. 2011;28:2731–9.

Tang YX, Jin J, Hu DW, Yong ML, Xu Y, He LP. Elucidation of the infection process of *Ustilaginoidea virens* (teleomorph: *Villosiclava virens*) in rice spikelets. Plant Pathol. 2013;62:1–8.

Wu J, Kou YJ, Bao JD, Li Y, Tang MZ, Zhu XL, et al. Comparative genomics identifies the *Magnaporthe oryzae* avirulence effector AvrPi9 that triggers Pi9-mediated blast resistance in rice. New Phytol. 2015;206:1463–75.

Xin XF, Nomura K, Aung K, Velásquez AC, Yao J, Boutrot F, et al. Bacteria establish an aqueous living space in plants crucial for virulence. Nature. 2016;539:524–9.

Yong ML, Fan LL, Li DY, Liu YJ, Cheng FM, Xu Y, et al. *Villosiclava virens* infects specifically rice and barley stamen filaments due to the unique host cell walls. Microsc Res Tech. 2016;79:838–44.

Yu M, Yu J, Hu J, Huang L, Wang Y, Yin X, et al. Identification of pathogenicity-related genes in the rice pathogen *Ustilaginoidea virens* through random insertional mutagenesis. Fungal Genet Biol. 2015;76:10–9.

Zhang LL, Ma XF, Zhou BB, Zhao JQ, Fan J, Fu H, et al. EDS1-mediated basal defense and SA-signaling contribute to postinvasion resistance against tobacco powdery mildew in *Arabidopsis*. Physiol Mol Plant Pathol. 2015;91: 120–30.

Zhang Y, Zhang K, Fang A, Han Y, Yang J, Xue M, et al. Specific adaptation of *Ustilaginoidea virens* in occupying host florets revealed by comparative and functional genomics. Nat Commun. 2014;5:3849.

Zhao ZX, Xu YB, Wang TT, Ma XF, Zhao JQ, Li Y, et al. Proper expression of AS1 is required for RPW8.1-mediated defense against powdery mildew in Arabidopsis. Physiol Mol Plant Pathol. 2015;92:101–11.

Zheng D, Yi W, Yu H, Xu JR, Wang C. *UvHOG1* is important for hyphal growth and stress responses in the rice false smut fungus *Ustilaginoidea virens*. Sci Rep. 2016;6:24824.

Zheng MT, Ding H, Huang L, Wang YH, Yu MN, Zheng R, et al. Low-affinity iron transport protein Uvt3277 is important for pathogenesis in the rice false smut fungus *Ustilaginoidea virens*. Curr Genet. 2017;63:131–44.